Difference frequency generation in the mid-infrared with orientation-patterned gallium phosphide crystals

Difference frequency generation in the mid-infrared with orientation-patterned gallium phosphide crystals

GIACOMO INSERO[1,2], CECILIA CLIVATI[3,*], DAVIDE D'AMBROSIO[3], PAOLO DE NATALE[1,2], GABRIELE SANTAMBROGIO[1,2,3], PETER G. SCHUNEMANN[4], JEAN-JACQUES ZONDY[5], AND SIMONE BORRI[1,2]

[1]*Istituto Nazionale di Ottica, INO-CNR, and European Laboratory for Nonlinear Spectroscopy, LENS, via N. Carrara 1, 50019 Sesto Fiorentino, Italy*
[2]*Istituto Nazionale di Fisica Nucleare,INFN, Sezione di Firenze, via G. Sansone 1, 50019 Sesto Fiorentino, FI, Italy*
[3]*Istituto Nazionale di Ricerca Metrologica, INRIM, Strada delle Cacce 91, 10135 Torino, Italy*
[4]*BAE Systems, Inc., MER15-1813, P.O. Box 868, Nashua, NH, USA 03061-0868*
[5]*Nazarbaev University, School of Science and Technology, Physics Department, Kabanbay Batyr 53, 010000 Astana, Kazakhstan*
**Corresponding author: c.clivati@inrim.it*

Received XX Month XXXX; revised XX Month, XXXX; accepted XX Month XXXX; posted XX Month XXXX (Doc. ID XXXXX); published XX Month XXXX

We report on the generation of coherent mid-infrared radiation around 5.85 μm by difference frequency generation (DFG) of continuous-wave Nd:YAG laser at 1064 nm and diode-laser at 1301 nm in an orientation-patterned gallium phosphide (OP-GaP) crystal. We provide the first characterization of the linear, thermo-optic and nonlinear properties of OP-GaP in a DFG configuration. Moreover, by comparing the experimental efficiency to Gaussian beam DFG theory, we derive an effective nonlinear coefficient *d* = 17(3) pm/V for first-order quasi-phase-matched OP-GaP. The temperature and signal-wave tuning curves are in qualitative agreement with theoretical modeling. © 2015 Optical Society of America

***OCIS codes**: (190.4410) Nonlinear optics, parametric processes; (160.4330) Nonlinear optical materials; (140.6810) Thermal effects; (140.3070) Infrared and far-infrared lasers.*

http://dx.doi.org/10.1364/OL.99.099999

Tunable single-frequency and powerful laser sources are needed for both sensitive and precision molecular spectroscopy in the mid-infrared (MIR) [1]. Quantum cascade lasers (QCLs) are available over the whole wavelength range and produce radiation with up to hundreds of mW. However, their free-running linewidths range from a few to tens of MHz [2]. Thus, for precision spectroscopy, coherent radiation traceable to primary frequency standards must be produced to either phase lock or injection lock such QCLs [3,4].

Continuous-wave (cw) optical parametric oscillators (OPOs) combine single-frequency and powerful emission [5]. However, cw OPOs have only been demonstrated at wavelengths below 5 μm, where oxide birefringent materials ($LiNbO_3$, $KTiOPO_4$…) are transparent. Non-oxide materials, like $AgGaSe_2$, $LiInSe_2$, $CdSiP_2$ [6], show larger residual absorption loss compared to oxide materials, and therefore only with silver gallium sulfide ($AgGaS_2$) genuinely cw emission could be demonstrated at 2.5 μm [7]. Among the recently developed quasi phase-matched III-V semiconductors (OP-GaAs, OP-GaP [8,9]), only *quasi*-cw parametric oscillation at 4.7 μm has been reported for OP-GaAs, albeit at a pump wavelength of 2.1 μm (Ho:YAG) where absorption is much lower than at 1064 nm.

An alternative method to produce narrow-linewidth, widely-tunable, μW-to-mW level MIR coherent radiation is DFG [10]. Yet again, commercial crystals such as $LiNbO_3$ and $LiTaO_3$ are transparent only below 5 μm. For longer wavelengths, quasi-phase-matched (QPM) OP-GaAs or OP-GaP are preferable for DFG over birefringence phased-matched chalcogenides because they are free from spatial walk-off, which dramatically reduces the nonlinear interaction length. While down-conversion schemes using OP-GaAs have been extensively investigated, to date still few works have been devoted to the newly developed orientation-patterned gallium phosphide (OP-GaP) [11]. The advantages of OP-GaP over OP-GaAs are the larger thermal conductivity and the larger bandgap energy that is better suited for pumping at the convenient Nd:YAG wavelength of 1064 nm [6].

In this Letter, we provide the first characterization of DFG in OP-GaP and report on its linear, thermo-optic and nonlinear properties. We used a single-frequency Nd:YAG laser (λ_p=1064.5 nm, Mephisto MOPA, Coherent Inc, $\Delta\nu \approx$10 kHz, hereafter called pump) and an extended-cavity tunable diode laser (λ_s=1301.1 nm, DL 100, Toptica Photonics AG, $\Delta\nu \approx$100 kHz, hereafter called signal).

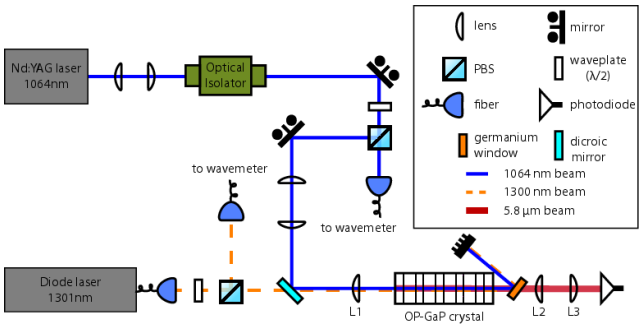

Fig. 1. Experimental DFG laser setup. After the Ge window, L2 (f=50 mm) collects the idler and L3 focuses it on the 200-μm active area of the HgCdTe detector. L2 and L3 are made of CaF_2.

Up to 65 μW of single-frequency idler at λ_i=5.85 μm were generated from ~10 W of pump and ~40 mW of signal in a 24.6 mm long QPM structure, limited by thermal dephasing effects arising from the non-negligible absorption at the pump and signal wavelengths. An effective first-order QPM nonlinear coefficient $d = (2/\pi)d_{14}$ =17(3) pm/V has been evaluated from the absolute measurement of DFG conversion efficiency versus focusing, and these results are in agreement with cw Gaussian beam DFG theory [12]. Moreover, the measured spectral and temperature curve bandwidths validate a recently proposed temperature-dependent Sellmeier equation for GaP [11].

The DFG setup is shown in Fig.1. Pump and signal laser beams are nearly TEM_{00}. They are coaxially focused in the OP-GaP crystal using a lens, L1. Four different focal lengths have been tried for L1: 150, 100, 75, and 50 mm. A variable telescope on the pump path allows for matching the beam waist of the pump to that of the signal, and superimposing the two waists inside the crystal longitudinally during the idler power optimization. The waists $w_{p,s}$ were accurately measured (Table 1) using the calibrated pinhole transmission technique (±10% error) [13]. The measurements satisfied the diffraction-limited formula $w=(4/\pi)\lambda f/D$, where D is the beam diameter, with a ratio $w_s/w_p \approx \lambda_s/\lambda_p$. Although such a waist ratio does not correspond to the equal confocal parameter focusing condition, which theoretically yields optimal efficiency [12], it is sufficiently close to it. After the crystal, the idler beam is separated from the near-IR pump and signal beams using a coated Ge window and refocused on a thermo-electrically cooled HgCdTe photodetector (VIGO system, PVI-4TE-5/MIP-DC-10M) using a couple of 50 mm lenses, L2 and L3. The detector absolute responsivity was calibrated by simultaneously measuring the power of a QCL at 5.85 μm in a range ~ 2-70 μW with a calibrated radiometer.

Table 1. Experimental values of the waists for pump (w_p) and signal (w_s), measured with the calibrated pinhole transmission technique (±10% uncertainty), for the four focal lengths used for L1. Calculated idler waist $w_i = w_p w_s / \left[w_p^2 + w_s^2\right]^{1/2}$ and Rayleigh range $z_i = (1/2) k_i w_i^2$, where $k_i = 2\pi n_i / \lambda_i$ is the idler wavevector and n_i = 3.18 is the GaP refractive index at the idler wavelength [14].

f (mm)	w_p (μm)	w_s (μm)	w_i (μm)	z_i (mm)
150	67.5	82.5	52.24	4.67
100	45	55	34.83	2.07
75	27	33	20.90	0.75
50	19	23	14.65	0.37

An OP-GaP crystal with length l_c = 24.6 mm and anti-reflection-coated at the 3 wavelengths on both facets (reflections at the three wavelengths is below 1%) was characterized. The OP structure was grown by polar-on-nonpolar molecular beam epitaxy, lithographically patterned, reactive ion-etched and regrown to yield templates for subsequent bulk growth by low-pressure hydride vapor phase epitaxy [8,11]. The crystal carried a 400-μm-thick melt-grown substrate, over which the OP layer extends for another 400 μm thickness. The overall thickness of the chip is ~1.5 mm, with a ~ 6 mm wide OP layer carrying a 50% duty cycle periodic domain reversal (grating period Λ = 24 μm). The sample is housed in a massive copper-block oven whose temperature is regulated by a P-I servo-controller, and the oven is mounted on a *XYZ*-θφ positioner for DFG efficiency optimization. The phase-matching temperature was found to be around T = 43°C.

The absorption of the sample was measured at pump and signal frequencies, yielding average absorption coefficients $\alpha_p \approx 0.17$ cm^{-1} and $\alpha_s \approx 0.12$ cm^{-1} inside the 400-μm thick OP region. Instead, much larger coefficients were found in the substrate ($\alpha_p \approx 0.58$ cm^{-1} and $\alpha_s \approx 0.53$ cm^{-1}) , which are likely due to contaminations that are not present in the high-purity vapor-grown OP region. For the idler absorption coefficient, the value $\alpha_i \approx 0.007$ cm^{-1} measured with a Perkin Elmer Spectrum GX FTIR was assumed [11]. The pump and signal waves were polarized vertically (along the [001] crystallographic axis) and horizontally (along [110]) respectively, which yielded horizontally polarized idler radiation. This configuration ensures full coupling of the d_{14} nonlinear coefficient of III-V semiconductors [14].

Figure 2 displays the absolute MIR power generated just after the crystal as a function of the pump power, for a fixed signal wave power P_s ~ 40 mW. Each curve corresponds to the focusing conditions summarized in Table 1. The maximum idler power P_i ~ 65 μW is generated at P_p ~ 10 W at the strongest focusing (f = 50 mm) although the curve for f =75 mm almost overlaps the f = 50 mm curve, meaning that these focal lengths must be around the optimum to saturate the DFG efficiency.

The limited transparency of GaP at 1064 nm results in heating of the crystal; the thermo-optic effect consequently changes the refractive index, affecting the QPM conditions.

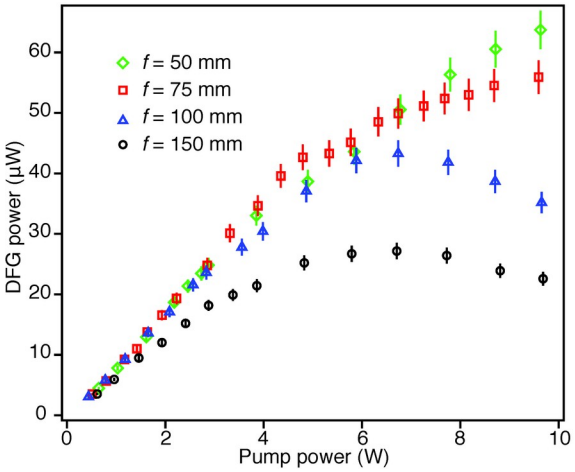

Fig. 2. Idler power at λ_i =5.85 μm versus pump power. The signal power at 1301.1 nm was kept constant at ~40 mW and the temperature of the crystal was optimized for each point.

This is then responsible for two observed effects. First, at the largest powers, the pump beam heats the crystal by several degrees above the oven temperature, shifting the crystal temperature out of the QPM condition. In our measurements we took into account this process by adjusting the oven temperature, so that each data point in Fig. 2 corresponds to the optimal QPM condition, once thermal equilibrium is reached. Second, the finite thermal conductivity of GaP yields a transverse temperature gradient. This affects the QPM condition in a spatial-dependent fashion. While the QPM condition is well satisfied for weak pump powers, for substantial thermal load it cannot be satisfied throughout the whole beams volume. This accounts for the observed idler power saturation at larger pump powers, whereas a linear behavior would be expected from Gaussian beam DFG theory, with slope $\Gamma=P_i/(P_p P_s)$, known as conversion efficiency [12].

To evaluate the effective nonlinear coefficient d, only the linear portions of the curves from Fig. 2 were used, so as to exclude thermal effects from the analysis. Furthermore, we have considered only the f = 100 and 150 mm loose focusing data for which the modes of all three waves are confined within the active QPM layer volume, for reasons which will be stated further. The effective nonlinear coefficient d is proportional to $\sqrt{\Gamma}$ and is obtained by applying the analysis described in ref. [12], using Gaussian beam DFG theory and taking absorption into consideration. The result is shown in Fig. 3 as a solid line, where the conversion efficiency Γ is plotted against the focusing parameter $l=l_c/z_i$, the crystal length expressed in units of Rayleigh length of the idler. The best match to the loose focusing experimental data is found for d=17(3) pm/V. The linear efficiency saturation observed for the two strong focusing data can be related to the limited thickness (400 μm) of the patterned layer. Indeed, the far field divergence angle of each wave is $\delta=\lambda/\pi n w_0$. For pump and signal, one finds that in all four focusing configurations (see Table 1) the beams are well inside the patterned layer over the whole length of the crystal.

Fig. 3: Conversion efficiency $\Gamma = P_i/(P_p P_s)$. The solid line represents the optimized theoretical efficiency calculated with the waist ratio $w_s/w_p=\lambda_s/\lambda_p$.

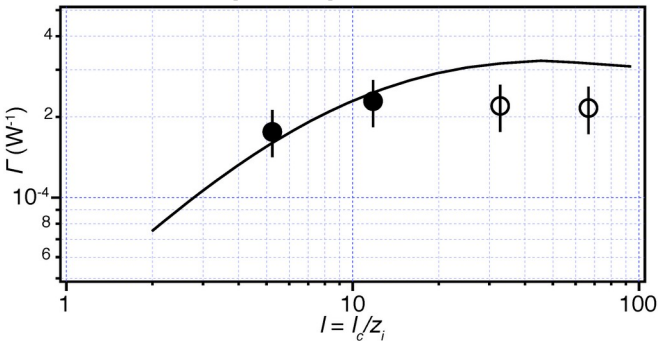

However, due to its longer wavelength, this is not the case for idler wave whose mean diameter at the output facet is evaluated to be 980 and 686 μm with f = 50 and 75 mm, respectively. For the two looser focusing cases, instead, the idler mode diameter remains within the 400 μm thickness of the patterned layer. Thus, for strong focusing, part of the generated idler expands outside the OP layer into the bulk region where the absorption is larger and QPM is no longer satisfied. Consequently the difference between the idler's phase and the sum-phase of pump and signal is not strictly identical within and outside the QPM layer, affecting thus the overall phase coherence of the DFG process along the crystal at strong focusing compared to the looser focusing cases where all three waves remain quasi phase-matched over the whole crystal length. How strong focusing affects the saturation of the generated DFG power could be checked by using a sample with identical length but with a thicker OP layer (e.g. 1000 μm).

It is interesting to compare the measured absolute effective nonlinear coefficient $d=(2/\pi)d_{14}$ to values of the $d_{14}(\equiv d_{36})$ coefficient of GaP derived from non-phase-matched second-harmonic generation. Levine reported $d_{14}=37(2)$ pm/V from Maker-fringe technique at 10.6 μm, $d_{14}=49(9)$ and 47(10) pm/V from wedge technique at 1.32 μm and 2.12 μm, respectively [15]. More recently, Shoji et al. accurately measured $d_{14}=38.6(4)$ pm/V from

wedge technique at 1.32 μm taking account of multiple reflection effects [16]. Note that the measurements by Levine have been rescaled to lower values following the standardization recommendation by Roberts [17]. Applying the Miller's rule factor $M_{14}=\prod_{i=1}^{3}\left(n^2(\lambda_i)-1\right)/\left(n^2(\Lambda_i)-1\right)$, where the Λ_i are Shoji's reference second-harmonic generation wavelengths and using a recently determined temperature-dependent Sellmeier equation to account for dispersion [11], one finds M_{14} = 0.82 for our DFG wavelengths, and thus a nonlinear coefficient d_{14} = 31.6 pm/V for 5.85 μm generation. For first-order QPM, this yields d = 20(2) pm/V, close to our experimental value d = 17(3)pm/V.

We have investigated the DFG tuning curves in dependence of signal wavelength and crystal temperature. We compared the experimental acceptance curves with the theoretical curves obtained from Gaussian beam DFG theory, where the appropriate phase-mismatch is retrieved by applying the Sellmeier equation from Ref. [11]. Figure 4 compares the experimental and theoretical temperature curves and Figure 5 the spectral tuning curve when the signal laser is tuned around the phase-matched wavelength. Data are shown for f = 150 mm and f = 75mm, and they are compared with the predictions from simple plane-wave and Gaussian beam DFG theory. Broadening and asymmetry of the tuning curves for both focusing conditions are qualitatively in agreement with focused-beam DFG theory. Moreover, the side lobes in the tuning curves predicted by plane-wave theory are washed out by beam aperture effects. At looser focusing there is a good match between experiments and theory, both for temperature and spectral acceptance bandwidths, validating thus the thermo-optical dispersion relation given in Ref. [11]. The calculations shown in Figure 5 take water absorption from the atmosphere into account (HITRAN data for standard atmosphere; 10 cm beam path length [18]).

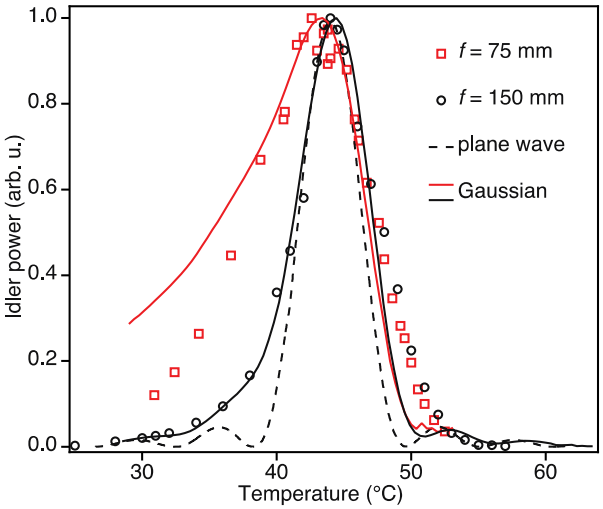

Fig. 4. Measured temperature tuning curves for loose and strong focusing conditions (symbols) compared with results from theoretical model.

In conclusion, we reported on the first complete characterization of the cw difference-frequency generation process in an OP-GaP crystal, and demonstrate DFG at 5.85 μm. The maximum generated idler power of ~ 65 μW is limited by thermal effects arising from the substantial absorption at 1064 nm by the OP-GaP samples. As the absorption coefficients of OP-GaP for wavelengths beyond 1.5 μm are about one order of magnitude lower than at 1064 nm, a pump laser in the telecom band around 1550 nm would allow to increase significantly the idler power (diode lasers for the signal around 2 μm are commercially available). The generated radiation can be referred to an absolute frequency standard by locking the pump and signal lasers to a near-IR comb, and the narrow-linewidth DFG radiation is sufficient to phase-lock a broader-linewidth QCL.

Funding. The ELI European project; INFN (SUPREMO); EMPIR-15SIB05-OFTEN, which has received funding from the EMPIR programme co-financed by the Participating States and from the European Union's Horizon 2020 research and innovation programme.

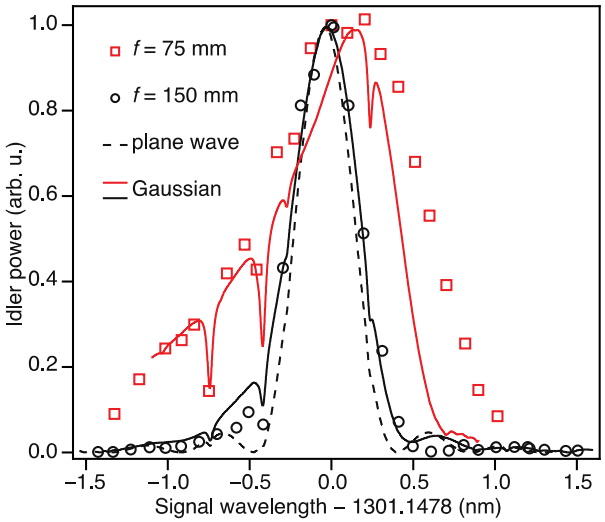

Fig. 5. Measured signal tuning curves for loose and strong focusing (symbols) and results from theoretical model.

References

1. S. Borri and G. Santambrogio, Adv. in Phys.: X, (2016), doi: 10.1080/23746149.2016.1203732
2. S. Bartalini, S. Borri, I. Galli, G. Giusfredi, D. Mazzotti, T. Edamura, N. Akikusa, M. Yamanishi, and P. De Natale, Opt. Expr. 19, 17996 (2011).
3. S. Borri, I. Galli, F. Cappelli, A. Bismuto, S. Bartalini, P. Cancio, G. Giusfredi, D. Mazzotti, J. Faist, and P. De Natale, Opt. Lett. 37, 1011 (2012)

4. I. Galli, M. Siciliani de Cumis, F. Cappelli, S. Bartalini, D. Mazzotti, S. Borri, A. Montori, N. Akikusa, M. Yamanishi, G. Giusfredi, P. Cancio, and P. De Natale, Appl. Phys. Lett. 102, 121117 (2013)
5. I. Ricciardi, E. De Tommasi, P. Maddaloni, S. Mosca, A. Rocco, J.-J. Zondy, M. De Rosa, and P. De Natale, Opt. Express 20, 9178 (2012)
6. V. Petrov, Prog. Quantum Electron. 42, 1 (2015)
7. A. Douillet and J.-J. Zondy, Opt. Lett. 23, 1259 (1998)
8. V. Tassev, M. Snurea, R. Petersona, K. L. Scheplera, R. Bedforda, M. Manna, S. Vangalab, W. Goodhuec, A. Lind, J. Harrisd, M. Fejerd, and P. Schunemann, Proc. SPIE 8604, 86040V (2013)
9. L. Pomeranz, P. Schunemann, S. Setzler, C. Jones, P. Budni, CLEO 2012, paper JTh1I.4, OSA Technical Digest, doi:10.1364/CLEO_AT.2012.JTh1I.4
10. I. Galli, S. Bartalini, P. Cancio, G. Giusfredi, D. Mazzotti, and P. De Natale, Opt. Express 17, 9582 (2009)
11. L. A. Pomeranz, P. G. Schunemann, D. J. Magarrell, J. C. McCarthy, K. T. Zawilski, and D. E. Zelmon, Proc. SPIE 9347, 93470K (2015)
12. J.-J. Zondy, Opt. Commun. 149, 181 (1998)
13. J.-J. Zondy, D. Touahri, and O. Acef, J. Opt. Soc. Am. B 14, 2481 (1997)
14. P. Kuo, PhD dissertation, http://nlo.stanford.edu/content/thick-film-orientation-patterned-gallium-arsenide-nonlinear-optical-frequency-conversion
15. Z. H. Levine, Phys. Rev. B 49, 4532 (1994)
16. I. Shoji, T. Kondo, A. Kitamoto, M. Shirane, and R. Ito, J. Opt. Soc. Am. B 14, 2268 (1997)
17. D. A. Roberts, IEEE J. Quantum Electron. 28, 2057 (1992)
18. http://hitran.iao.ru/.

Full References with titles

1. S. Borri and G. Santambrogio, *Laser spectroscopy of cold molecules*, Adv. in Phys.: X, (2016), DOI: 10.1080/23746149.2016.1203732
2. S. Bartalini, S. Borri, I. Galli, G. Giusfredi, D. Mazzotti, T. Edamura, N. Akikusa, M. Yamanishi, and P. De Natale, "Measuring frequency noise and intrinsic linewidth of a room-temperature DFB quantum cascade laser", Opt. Expr. 19, 17996 (2011).
3. S. Borri, I. Galli, F. Cappelli, A. Bismuto, S. Bartalini, P. Cancio, G. Giusfredi, D. Mazzotti, J. Faist, and P. De Natale, *Direct link of a mid-infrared QCL to a frequency comb by optical injection*, Opt. Lett. **37**, 1011 (2012).
4. I. Galli, M. Siciliani de Cumis, F. Cappelli, S. Bartalini, D. Mazzotti, S. Borri, A. Montori, N. Akikusa, M. Yamanishi, G. Giusfredi, P. Cancio, and P. De Natale, *Comb-assisted subkilohertz linewidth quantum cascade laser for high-precision mid-infrared spectroscopy*, Appl. Phys. Lett. **102**, 121117 (2013)
5. I. Ricciardi, E. De Tommasi, P. Maddaloni, S. Mosca, A. Rocco, J.-J. Zondy, M. De Rosa and P. De Natale, *Frequency-comb-referenced singly-resonant OPO for sub-Doppler spectroscopy,* Opt. Express **20**, 9178 (2012)
6. V. Petrov, *Frequency down-conversion of solid-state laser sources to the mid-infrared spectral range using non-oxide nonlinear crystals*, Prog. Quantum Electron. **42**, 1 (2015)
7. A. Douillet and J.-J. Zondy, *Low-threshold, self-frequency-stabilized $AgGaS_2$ continuous-wave subharmonic optical parametric oscillator*, Opt. Lett. **23**, 1259 (1998)
8. V. Tassev, M. Snurea, R. Petersona, K. L. Scheplera, R. Bedforda, M. Manna, S. Vangalab, W. Goodhuec, A. Lind, J. Harrisd, M. Fejerd, and Peter Schunemann, *Progress in orientation-patterned GaP for next-generation nonlinear optical devices*, Proc. of SPIE Vol. **8604**, 86040V (2013)
9. L. Pomeranz, P. Schunemann, S. Setzler, C. Jones, and P. Budni, *Continuous-wave Optical Parametric Oscillator based on Orientation Patterned Gallium Arsenide (OP-GaAs)*, CLEO 2012, paper JTh1I.4, OSA Technical Digest, doi:10.1364/CLEO_AT.2012.JTh1I.4
10. I. Galli, S. Bartalini, P. Cancio, G. Giusfredi, D. Mazzotti, and P. De Natale, "Ultra-stable, widely tunable and absolutely linked mid-IR coherent source", Opt. Express 17, 9582 (2009)
11. L. A. Pomeranz, P. G. Schunemann, D. J. Magarrell, J. C. McCarthy, K. T. Zawilski, and D. E. Zelmon, *1-μm-pumped OPO based on orientation-patterned GaP*, Proc. SPIE **9347**, 93470K (2015)
12. J.-J. Zondy, *The effects of focusing in type-I and type-II difference-frequency generations*, Opt. Commun. **149**, 181 (1998)
13. J.-J. Zondy, D. Touahri, and O. Acef, *Absolute value of the d_{36} nonlinear coefficient of $AgGaS_2$: Prospect for a low-threshold doubly resonant oscillator-based 3:1 frequency divider*, J. Opt. Soc. Am. B **14**, 2481 (1997)
14. P. Kuo, PhD dissertation, http://nlo.stanford.edu/content/thick-film-orientation-patterned-gallium-arsenide-nonlinear-optical-frequency-conversion
15. Z. H. Levine, *Optical second-harmonic susceptibilities: Frequency-dependent formulation with results for GaP and GaAs*, Phys. Rev. B **49**, 4532 (1994)
16. I. Shoji, T. Kondo, A. Kitamoto, M. Shirane, and R. Ito, *Absolute scale of second-order nonlinear-optical coefficients* ,J. Opt. Soc. Am. B **14**, 2268 (1997)
17. D. A. Roberts, *Simplified Characterization of Uniaxial and Biaxial Nonlinear Optical Crystals: A Plea for Standardization of Nomenclature and Conventions*, IEEE J. Quantum Electron. **28**, 2057 (1992)
18. http://hitran.iao.ru/.